Matrix Biology 125 (2024) 1–11

Contents lists available at ScienceDirect

Matrix Biology

journal homepage: www.elsevier.com/locate/matbio

Peroxidasin is required for full viability in development and for maintenance of tissue mechanics in adults

K. Elkie Peebles [a,b,c], Kimberly S. LaFever [a,b], Patrick S. Page-McCaw [a,c,d], Selene Colon [c,d], Dan Wang [e], Aubrie M. Stricker [a,b,c], Nicholas Ferrell [e], Gautam Bhave [c,d,*], Andrea Page-McCaw [a,b,c,*]

[a] Department of Cell and Developmental Biology, Vanderbilt University, Nashville, TN, United States
[b] Program in Developmental Biology, Vanderbilt University, Nashville, TN, United States
[c] Center for Matrix Biology, Vanderbilt University Medical Center, Nashville, TN, United States
[d] Division of Nephrology, Department of Medicine, Vanderbilt University Medical Center, Nashville, TN, United States
[e] Division of Nephrology, Department of Internal Medicine, The Ohio State University Wexner Medical Center, Columbus, OH 43210, United States

ARTICLE INFO

Keywords:
Basal lamina
Sulfilimine bond
Extracellular matrix
Tensile stiffness
Dynamics
Homeostasis

ABSTRACT

Basement membranes are thin strong sheets of extracellular matrix. They provide mechanical and biochemical support to epithelia, muscles, nerves, and blood vessels, among other tissues. The mechanical properties of basement membranes are conferred in part by Collagen IV (Col4), an abundant protein of basement membranes that forms an extensive two-dimensional network through head-to-head and tail-to-tail interactions. After the Col4 network is assembled into a basement membrane, it is crosslinked by the matrix-resident enzyme Peroxidasin to form a large covalent polymer. Peroxidasin and Col4 crosslinking are highly conserved throughout the animal kingdom, indicating they are important, but homozygous mutant mice have mild phenotypes. To explore the role of Peroxidasin, we analyzed mutants in *Drosophila*, including a new CRISPR-generated catalytic null, and found that homozygotes were mostly lethal with 13 % viable escapers. Mouse mutants also show semi-lethality, with Mendelian analysis demonstrating ~50 % lethality and ~50 % escapers. Despite the strong mutations, the homozygous fly and mouse escapers had low but detectable levels of Col4 crosslinking, indicating the existence of inefficient alternative crosslinking mechanisms, probably responsible for the viable escapers. Fly mutant phenotypes are consistent with decreased basement membrane stiffness. Interestingly, we found that even after basement membranes are assembled and crosslinked in wild-type animals, continuing Peroxidasin activity is required in adults to maintain tissue stiffness over time. These results suggest that Peroxidasin crosslinking may be more important than previously appreciated.

Introduction

The basement membrane is a distinct sheet-like type of extracellular matrix found in virtually all animals, in nearly all tissues. Basement membranes underlie epithelia, and they surround muscles, nerves, blood vessels, and organs. In terms of function, basement membranes act as mechanical supports, reservoirs of signaling molecules, and signaling insulators [1,2]. Basement membranes are comprised of independent networks of laminin and type IV collagen, with other conserved proteins and proteoglycans assembling on these networks [3,4]. Type IV collagens (Col4) are highly abundant proteins in basement membranes [5], and these assemble into heterotrimers before secretion from the cell. Outside the cell, Col4 heterotrimers form a branched network by assembling with each other at their N- and C-termini with four heterotrimers assembling at the N-terminal 7S domain and two heterotrimers assembling at the C-terminal NC1 domain [6,7]. The collagen network determines much of the mechanical strength of the basement membrane because after Col4 is assembled in basement membranes, it is crosslinked to form a continuous large covalent network.

Head-to-head NC1 domains are covalently crosslinked by a chemical bond that appears unique for this purpose, a sulfilimine bond (S=N) that joins a hydroxylysine of an NC1 domain in one heterotrimer to a

* Corresponding authors at: Department of Cell and Developmental Biology, Vanderbilt University, Nashville, TN, United States, and Division of Nephrology, Department of Medicine, Vanderbilt University Medical Center, Nashville, TN, United States.
E-mail addresses: gautam.bhave@vumc.org (G. Bhave), andrea.page-mccaw@vanderbilt.edu (A. Page-McCaw).

https://doi.org/10.1016/j.matbio.2023.11.005
Received 17 August 2023; Received in revised form 6 November 2023; Accepted 21 November 2023
Available online 23 November 2023

methionine domain of the opposing heterotrimer [8]. Sulfilimine crosslinking is accomplished by the enzyme Peroxidasin, first discovered in *Drosophila* as an enzyme that localized to the basement membrane [9], a location now understood to be consistent with its function in crosslinking assembled basement membrane. In addition to crosslinking Col4, Peroxidasin has an immune function of killing gram negative bacteria in the lung through oxidation [10]. Like collagen IV, it is highly conserved throughout the animal kingdom [11]. Its role in Col4 crosslinking and its high degree of conservation suggested it would be an essential enzyme.

Given this expectation, it was surprising then when the first mouse mutant in *Peroxidasin, Pxdn*^{T3816A}, was reported to be homozygous viable with eye defects – anterior segment dysgenesis and micropthalmia – as the only prominent phenotype [12]. A second mutation

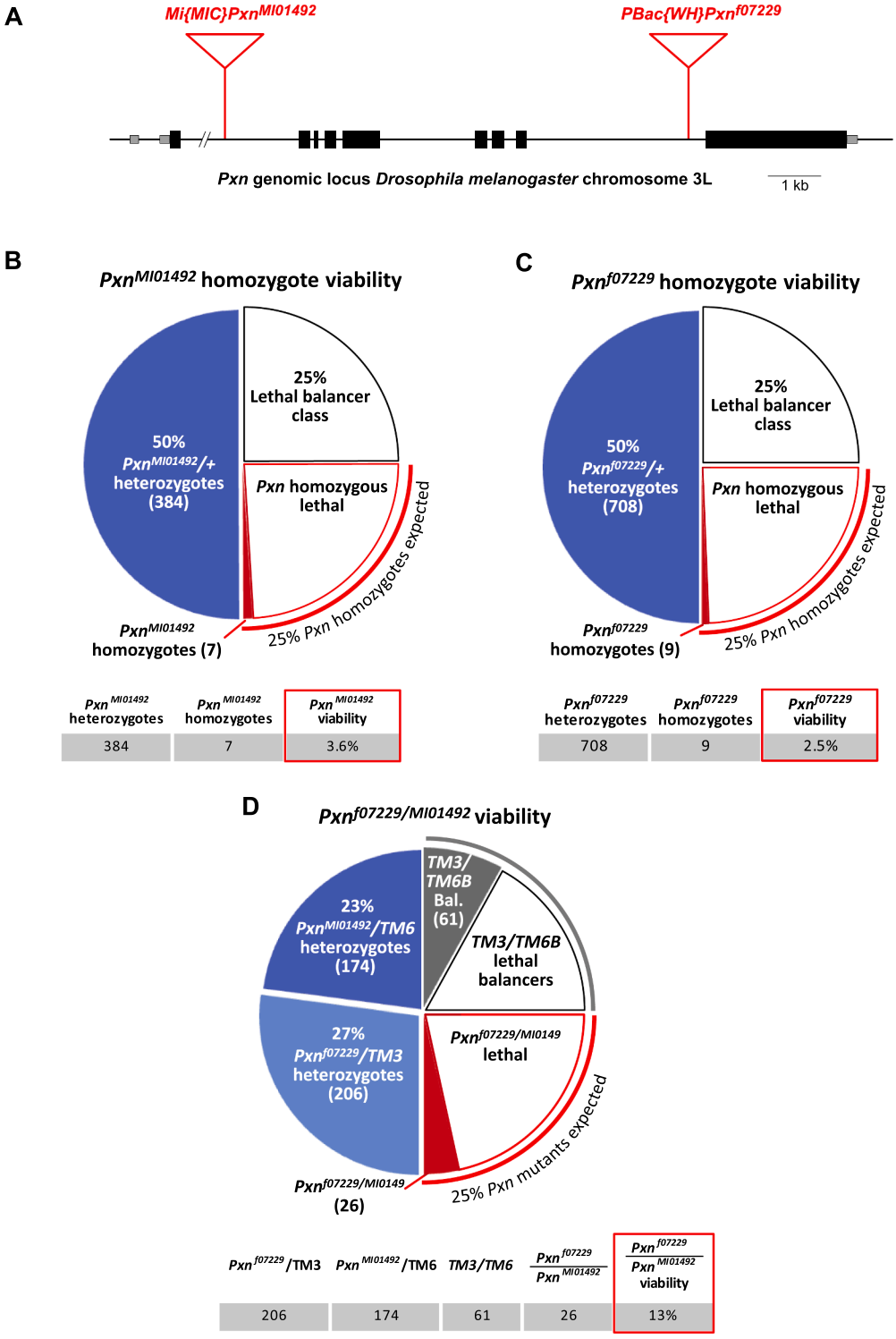

Fig. 1. Fly *Pxn* insertional mutants are semi-lethal.
A. Fly *Pxn* genomic locus. Exons indicated as black rectangles. Sites of transposon insertions generating loss-of-function mutations are indicated with red triangles. **B-D.** *Pxn* loss-of-function mutants have low viability to adulthood. All progeny were counted from **(B)** self-cross of *Pxn*^{MI01492}*/TM3,* **(C)** self-cross of *Pxn*^{f07229}*/TM6B*, or **(D)** the cross *Pxn*^{MI01492}*/TM3 x Pxn*^{f07229}*/TM6B*. 13 % of *Pxn*^{MI01492}*/Pxn*^{f07229} transheterozygotes are viable to adulthood.

was generated by CRISPR, deleting exon 1, and this mutant also had small eyes [13]. Indeed, human alleles of *Pxdn* have been identified in families with inherited eye defects [14,15]. These consistent phenotypes, apparently restricted to the anterior chamber of the eye, suggested that Pxdn had a limited role in matrix stability. A third mouse mutation in *Pxdn* was generated by homologous recombination, and homozygotes were tested directly for basement membrane stiffness. In line with its molecular function, $Pxdn^{K01}$ basement membranes were significantly and substantially less stiff in a tensional stiffness assay [16].

Peroxidasin mutants also exist in the fruitfly *Drosophila melanogaster* (where *Peroxidasin* is abbreviated *Pxn*), but there is no comprehensive report on *Pxn* mutant phenotypes. Because of the high sequence conservation between fly and mouse Peroxidasin, the *Drosophila* mutants may be useful for understanding its function. We began this study by analyzing the existing fly mutants. Surprised to find homozygous viable adults, we generated a catalytic null mutation in fly and compared its phenotype with two mouse knockout alleles. We find that in both species, *Peroxidasin* homozygotes are usually lethal, but even for the strongest catalytic null allele, some homozygous progeny survive. The fly phenotypes confirm the role of Pxn in tissue stiffness: homozygotes die during life stages with large mechanical strain, hatching and pupal eclosion; adults have dysmorphic gut muscles; and oocytes have more fragile basement membranes, demonstrated in an osmotic swelling assay. Finally, we use a tensile stiffness assay to demonstrate that even after basement membranes are assembled and cross-linked in wild-type animals, continuous Pxn function is required in adults to maintain tissue stiffness.

Results and discussion

Fly Peroxidasin mutants are lethal with incomplete penetrance

The Peroxidasin protein is ancient and highly conserved [11], so it is surprising that *Peroxidasin* (*Pxdn*) mutant mice are viable, with the only obvious phenotype being severe eye malformations [12,13,16]. To better understand the functions of Peroxidasin, we analyzed the lethality of two existing *Drosophila Peroxidasin* (*Pxn*) mutants, $Pxn^{MI01492}$ and Pxn^{f07229}. Both alleles are recessive loss-of-function, and they are caused by the insertion of two different transposons in two different *Pxn* introns (Fig. 1A). The coding region remains intact in these alleles, so the loss-of-function is caused by a reduction in gene product levels, similar to many other fly transposon alleles. Analyzing the progeny of heterozygous self-crosses, we counted a very small number of viable homozygotes for each allele, such that the apparent viability of *Pxn* homozygotes mutants was 3.6 % (*MI01492*) or 2.5 % (*f072229*) (Fig. 1B, C). However, when these insertion alleles were placed *in trans* so that a fly had one of each allele, viability improved: 13 % of $Pxn^{MI01492/f07229}$ mutants were viable (Fig. 1D). Because homozygous background effects were reduced in the trans-heterozygotes, 13 % viability is a better reflection of the lethal phenotype of these *Pxn* mutants.

We hypothesized that the 13 % viability of the trans-heterozygotes reflected residual function of the insertional alleles, and we expected that a *Pxn* catalytic null mutant would be a fully penetrant lethal mutation. Further, we expected *Pxn* null mutants to be embryonic lethal because basement membrane is first assembled in embryos [17,18]. To generate a null mutation, we targeted CRISPR guide RNAs to the sequence encoding the catalytic domain. The resulting mutation, Pxn^{11}, is a 727 bp deletion that generates a frame-shift, removing the C-terminus of protein. The missing region includes the proximal histidine (H1109) that directly contacts the heme iron [19], approximately half the amino acids found in the globular catalytic domain, the Cys residue at the C-terminal end of the catalytic domain that forms the trimer-stabilizing intermolecular disulfide bond, and the vWFC domain which mediates trimer assembly in the secretory system (Fig. 2A,B); based on its sequence, we conclude Pxn^{11} is a catalytic null mutation. Contrary to our expectations, Pxn^{11} homozygous mutants had similar

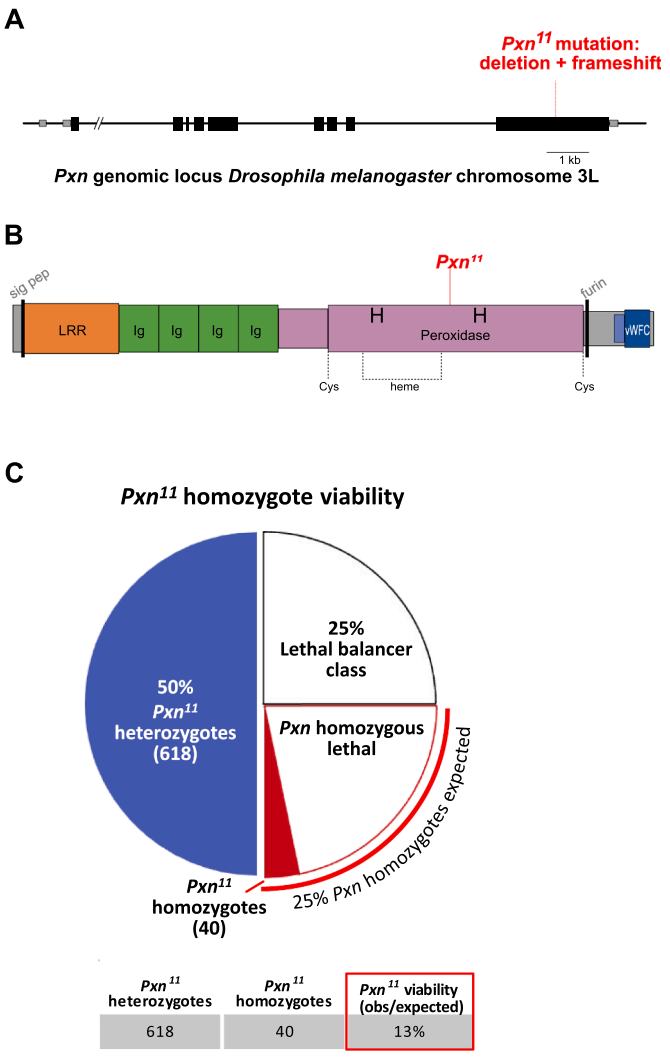

Fig. 2. The fly catalytic-null mutant Pxn^{11} is semi-lethal.
A. Fly *Pxn* genomic locus showing the start of the Pxn^{11} deletion and frameshift.
B. The Pxn^{11} mutation creates a deletion and frameshift that truncates the Pxn protein after residue 1040, as shown. Pxn protein domains: an N-terminal leucine rich repeat domain (LRR) and 4 immunoglobulin (Ig) domains precede the conserved peroxidase domain (purple). The heme co-factor is covalently coupled (dotted lines) to two residues. The distal histidine (H863) contacts the reactive peroxide, and the proximal histidine (H1109) contacts the catalytic iron, both indicated as H. The C-terminal region consists of a furin cleavage site, a coiled-coil domain (light blue), and a von Willebrand factor type C domain (vWFC, dark blue). These domains mediate peroxidasin trimerization, stabilized by an intersubunit disulfide bond between the indicated Cys residues; intra-subunit disulfide bonds are not indicated.
C. 13 % of Pxn^{11} homozygous catalytic-null mutants are viable to adulthood. Progeny were counted from self-crosses of $Pxn^{11}/TM3$.

viability as the $Pxn^{MI01492/f07229}$ transheterozygotes: 13 % of the homozygous animals survived while 87 % of them were lethal (Fig. 2C).

Mouse Peroxidasin mutations are lethal with incomplete penetrance

Given the fly catalytic null mutants were mostly lethal with some adult survivors, we wondered if there could be a similar range of viable/lethal progeny in mice. To address this question, we analyzed two mutant alleles at the mouse *Pxdn* locus. The first allele, designated $Pxdn^{K01}$, was generated by homologous recombination of the KOMP vector into the *Pxdn* gene locus, replacing the 9th exon with sequences that form a gene-trap, splicing to *LacZ* followed by polyadenylation

sequences to end transcription before the exon 9 sequence [20]. *K01* generates a predicted Pxdn protein that is truncated in the first Ig domain, which would have no catalytic function (Fig. 3A,B). *K01* was generated in B6/129 hybrid embryonic stem cells, and it was outcrossed separately into C57BL/6 and 129S2 backgrounds for 10 generations. In both backgrounds, viable homozygous mutant *Pxdn*$^{K01/K01}$ adults were observed, and they were blind with a defect in development of the anterior chamber of the eye, as we previously described [16]. To investigate whether *Pxdn* mutants were fully viable, we genotyped all the pups from multiple heterozygous crosses to identify the numbers of

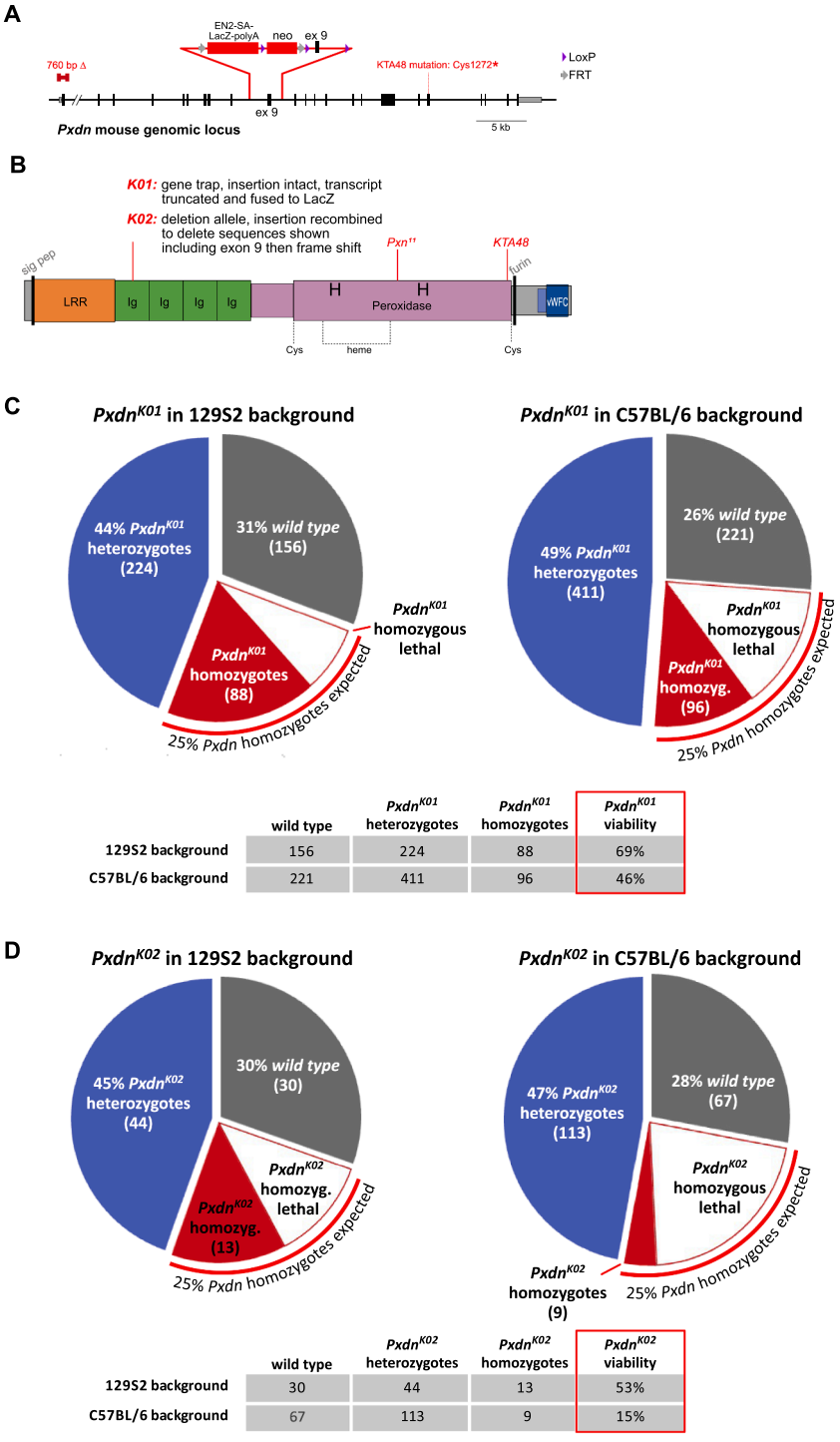

	wild type	PxdnK01 heterozygotes	PxdnK01 homozygotes	PxdnK01 viability
129S2 background	156	224	88	69%
C57BL/6 background	221	411	96	46%

	wild type	PxdnK02 heterozygotes	PxdnK02 homozygotes	PxdnK02 viability
129S2 background	30	44	13	53%
C57BL/6 background	67	113	9	15%

Fig. 3. Mouse *Pxdn* homozygotes are semi-lethal.
A. The mouse *Pxdn* genomic locus with previously reported and new mutations indicated. The 760 bp deletion of exon 1 was reported by Kim et al (2019), and the KTA48 mutation was reported by Yan et al (2014). Insertion of the KOMP vector, the parental line of the *K01* and *K02* mutants, is shown. See text for details.
B. The mouse Pxdn protein. The *K01* allele replaces the 9th exon with *LacZ* followed by polyadenylation sequences. The *K02* allele deletes the 9th exon, causing a frame shift. Protein domains are the same as for fly, described in Fig. 2. **C-D.** *Pxdn* mouse mutants have reduced viability to adulthood, even with different alleles in different genetic backgrounds. **(B)** In the 129S2 background, the viability of *Pxdn*^{K01} homozygous mutants to weaning is 69 % of expected, but in the C57BL/6 background, the viability of *Pxdn*^{K01} homozygous mutants to weaning is 46 % of expected. **(C)** In the 129S2 background, the viability of *Pxdn*^{K02} homozygous mutants to weaning is 53 % of expected, but in the C57BL/6 background, the viability of *Pxdn*^{K02} homozygous mutants to weaning is 15 % of expected.

each progeny class and compared them to Mendelian expectations. Fewer $Pxdn^{KO1/KO1}$ were detected post-weaning than expected, indicating that 69 % of $Pxdn^{KO1/KO1}$ mutants in the 129S2 background were viable (Fig. 3C). A chi-square test found the fraction of observed $Pxdn^{KO1/KO1}$ pups to be significantly different than the expected Mendelian ratio of 25 %, with $X^2 = 20.6$ with a corresponding p value < 0.0001 (Fig. S1). To determine whether this loss in viability was strain specific (*i.e.* caused by interactions with modifier alleles of other genes), the mutants were outcrossed to the C57BL/6 background and viability was again measured: in the C57BL/6 background only 46 % of $Pxdn^{KO1/KO1}$ mutants were viable.

The *KO1* allele is leaky and generates 7 % of the wild-type level of normal Pxdn transcripts [21]; for this reason it has been referred to as a KD allele [22]. Thus, we generated a second allele designated $Pxdn^{KO2}$, excising most of the inserted sequence including exon 9 sequence, by crossing sequentially to Flp and Cre recombinase lines. The $Pxdn^{KO2}$ allele was outcrossed separately into C57BL/6 and 129S2 backgrounds for 10 generations. The *KO2* homozygotes were 53 % viable in the 129S2 background; in the C57BL/6 background, *K02* had further reduced viability, with only 15 % of expected homozygotes surviving through weaning (Fig. 3D). For all four combinations of alleles and backgrounds, viability was significantly lower than expected as determined by chi-square test (Fig. S1). We conclude that, for both flies and mice, strong mutations in the *Peroxidasin* gene locus significantly reduce viability. In principle, the partial penetrance of the lethal phenotype could be caused by a mutation with residual catalytic function, or it could reflect a second source of variable low-level crosslinking. Because the fly mutation deletes the catalytic core of the protein, we ruled out the possibility of residual catalytic function and investigated the levels of crosslinking in these alleles.

Fly and mouse Peroxidasin mutants retain low levels of collagen IV NC1 crosslinking

Peroxidasin generates sulfilimine crosslinks between two head-to-head collagen IV NC1 domains in the basement membrane. The enzyme catalyzes the formation of hypobromous acid (HOBr) from bromide and hydrogen peroxide, and HOBr reacts with residues in an NC1 hexamer to generate sulfilimine bonds between Met93 of one NC1 and Hyl211 of the other, creating an NC1 dimer [23]. Because each NC1 domain contains both Met93 and Hyl211, a dimer can have one or two sulfilimine crosslinks, called D1 and D2 respectively, which migrate with different mobilities on polyacrylamide gel electrophoresis, or it can have zero crosslinks and remain a monomer (M), which runs with greatest mobility [23]. To investigate the extent of NC1 crosslinking in the new fly and mouse *Peroxidasin* mutants, we analyzed the level of D1, D2 and M by western blotting. We treated lysates from Pxn^{11} whole adult flies with collagenase to release the NC1 domain from the insoluble basement membrane and probed with a low-affinity antibody raised against fly NC1 [23]. In the Pxn^{11} mutant, the D2 double-crosslinked dimer was not observed; in contrast, the D1 single-crosslink band was reduced but clearly present (Fig. 4A). For the mouse mutants, we analyzed NC1 crosslinking in whole mouse kidneys (Fig. 4B). For the $Pxdn^{K01}$ homozygotes, as we reported previously [16], no D2 crosslinking was observed, and D1 crosslinking was reduced but still present, similar to the fly null results. For the new $Pxdn^{K02}$ allele, again D2 dimers were not observed, with reduced D1 crosslinking (Fig. 4B). Results from all three alleles in two species indicate that NC1 D1 crosslinking occurs at low levels even without Peroxidasin, perhaps reacting with the hypohalous acid products of myeloperoxidase or other related heme peroxidases, which exist in both mouse and fly. Alternatively, it is possible there is a low level of uncatalyzed reaction: for most enzymes this on-rate is too low to be detected given turnover, but in this case the crosslinked collagen products are long-lived, possibly enabling detection. Whatever the alternative source, this low level of crosslinking probably supports the partial viability of *Peroxidasin* mutants observed

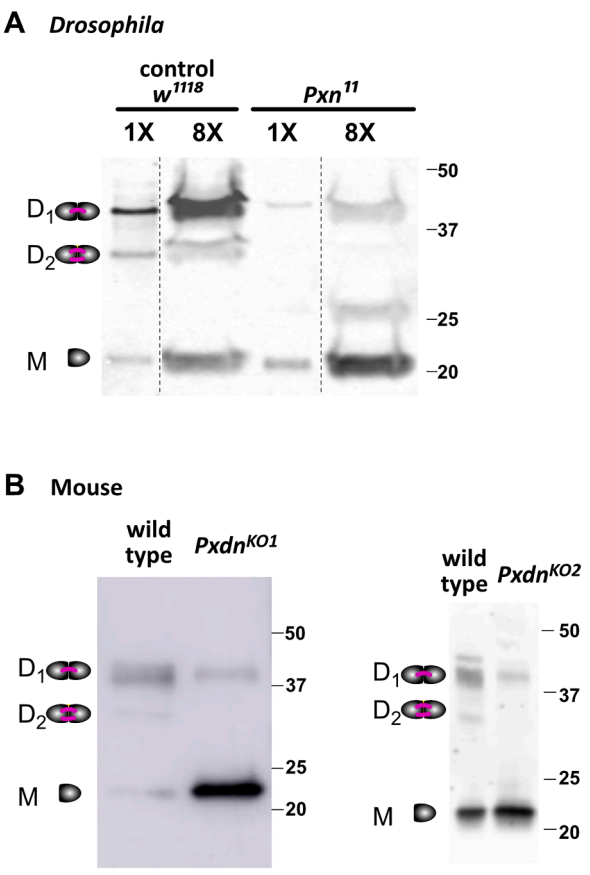

Fig. 4. Collagen IV NC1 crosslinking is reduced, but not absent, in fly and mouse mutants of *Peroxidasin*.
A. Western blot of whole adult flies homozygous for Pxn^{11} catalytic-null mutant shows dramatically decreased levels of NC1 domain crosslinking. Without Pxn catalytic activity, single crosslinks (D1) are still observed, but double crosslinks (D2) are not observed even when 8-fold more sample is probed. Crosslinking was probed by the mobility of NC1 domains, isolated by collagenase treatment of the insoluble fraction of fly lysate and probed by anti-NC1 antibody. Vertical lines represent omitted lanes.
B. Western blot of whole mouse kidneys homozygous for $Pxdn^{K01}$ or $Pxdn^{K02}$ show reduced NC1 crosslinking compared to wild-type. Crosslinking was probed with H22 antibody against the NC1 domain of Col4a2.

in both species. Thus, it may be reasonable to think of Peroxidasin as a specialist enzyme that promotes efficient crosslinking capable of generating a stable collagen network reinforced with double bonds, and without Peroxidasin there is a variably crosslinked suboptimal network that cannot reliably support life.

Peroxidasin mutants die at developmental periods when tissues exert force

To gain a better understanding of the requirements for Peroxidasin, we analyzed *Drosophila* Pxn^{11} mutants to determine when they died during development. The *Drosophila* life cycle comprises two distinct body plans, a worm-like larval body plan that develops during embryogenesis, and an adult fly body plan that develops during metamorphosis. Before metamorphosis, the larva grows through three distinct periods or instars, which can be recognized morphologically. We followed the development of hundreds of animals of three genotypes, Pxn^{11} homozygotes, $Pxn^{11}/TM3$ (heterozygous control for background effects), and w^{1118} (control with two wild-type *Pxn* alleles), tabulating their progression to the next stage of development. Although even controls showed some lethality before hatching, we found that 25–30 % fewer Pxn^{11} mutant embryos hatched compared to controls, a significant effect (Fig. 5A). The larval transitions were similar between Pxn^{11}

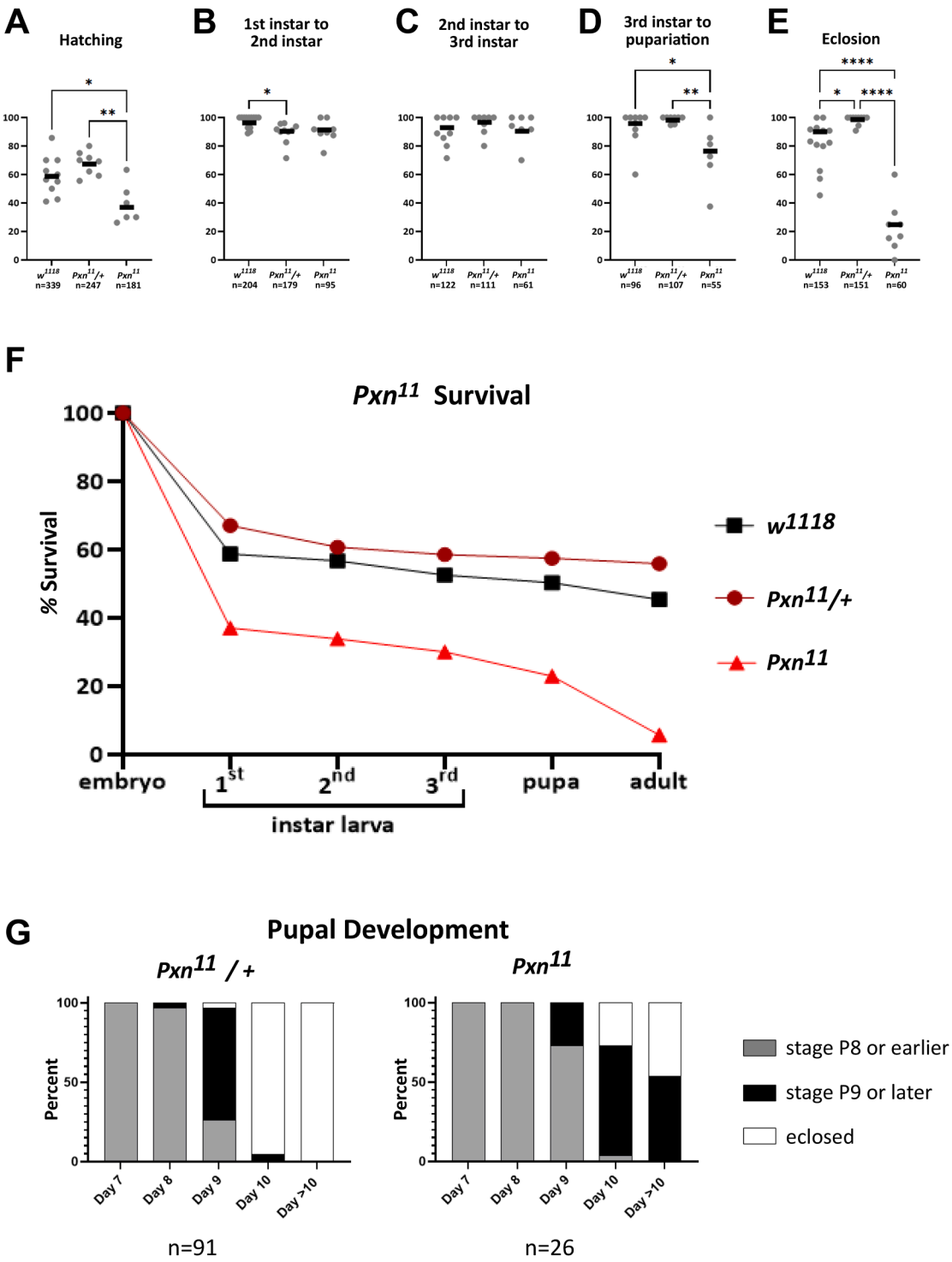

Fig. 5. ***Pxn11*** **mutants die at developmental stages that require mechanical force.**
A-E. Animals of indicated genotype were tracked across each developmental transition. Each individual data point is a % survival within a subpopulation (single vial). The bar represents the cumulative survival of the total number animals. *Pxn*^{11} mutants die most frequently during embryogenesis (A) and eclosion (E), both stages in which the animal must use force to break through either the eggshell or the pupal case.
F. Cumulative survival of animals shown in panels A-E.
G. *Pxn*^{11} mutant pupae appeared fully developed but could not escape the pupal case. *Pxn*^{11} mutant pupae older than 10 days never eclosed.

mutants and controls (Fig. 5B,C), followed by a slight, but significant, reduction in the ability of mutants to enter metamorphosis (pupariation, Fig. 5D). The largest lethal stage of *Pxn* mutants was observed at the transition from pupa to adult (eclosion), with *Pxn*^{11} pupae eclosing at only one quarter the rate of controls (Fig. 5E). The developmental lethality data is summarized in a survival curve in Fig. 5F. To investigate pupal lethality further, we observed the morphology of heterozygous and homozygous pupae and found that all *Pxn* homozygous animals, even those that failed to eclose, had fully formed adult bodies visible inside the pupal case (Fig. 5G).

Thus, *Pxn* mutants die most frequently during embryogenesis/hatching and eclosion. These stages require mechanical force, as

embryos and pupae both push through and break out of the enclosing cuticle, either eggshell or pupal case. Prior to both hatching and eclosion the animal generates large scale highly patterned motor programs which may place the tissues under considerable tension. The conclusion that *Pxn* mutants are less able to exert or withstand physical force is consistent with our understanding of *Pxn* as a collagen IV crosslinking enzyme.

We tried to analyze fertility in the surviving male and female homozygous Pxn^{11} mutants, and our initial observations were that they were almost completely sterile. However, we found that the sterility phenotype changed rapidly over the course of three months: testing laying frequency in small groups of homozygous Pxn^{11} females, we found that mutants from later generations laid dramatically more eggs, at about the same rate as controls (Fig. S2). These results indicate that Pxn^{11} mutants were under selection for suppressors of sterility, and because suppressors were rapidly generated, it suggests multiple genetic targets. To identify these suppressors, a future study could perform a genetic suppressor screen, but that is outside the scope of this study. The existence of readily available suppressor mutations or conditions may shed light on the crosslinking results and the partial viability.

Peroxidasin mutants are less stiff and fail under tensile strain

The requirement for *Pxn* during stages that require force suggested that *Pxn* mutants have altered tissue mechanics. Indeed, we previously showed that Pxn^{K01} kidney tubules have reduced stiffness in response to stretching, using an *ex vivo* assay to measure tensile stiffness [16]. In flies, we previously observed that the loss of *Pxn* by RNAi-based knockdown caused defects in muscle shape [24]. Here we confirmed that phenotype in Pxn^{11} homozygous mutants: on dissection of the adult midgut, we observed that the gut peristalsis muscles were dysmorphic (Fig. 6A,B), consistent with a mechanical role of basement membranes in distributing muscle force, an insight from research into muscular dystrophy [25].

Another basement membrane mechanics assay that has been utilized in *Drosophila* is the oocyte bursting assay. Oocytes develop inside a collagen IV basement membrane, and when immature oocytes are submerged *ex vivo* in hypo-osmotic water, the oocytes swell, placing the basement membrane under mechanical strain. After several minutes in hypo-osmotic media, oocytes may burst; the frequency and timing of bursting has been correlated with basement membrane stiffness as measured by atomic force microscopy [26], suggesting that oocyte bursting is caused by failure of the basement membrane. Within 10 minutes in water, Pxn^{11} mutants burst more frequently than control w^{1118} oocytes: whereas only 18 % of controls burst within 10 minutes, 73 % of Pxn^{11} mutants burst (Fig. 6C-E). This bursting rate is consistent with previous reports of oocyte bursting in basement membrane knockdowns [26]. Thus, analysis of the new Pxn^{11} null allele revealed developmental phenotypes, muscle phenotypes, and increased oocyte bursting rates, all showing that *Pxn* is important for establishing basement membrane mechanics.

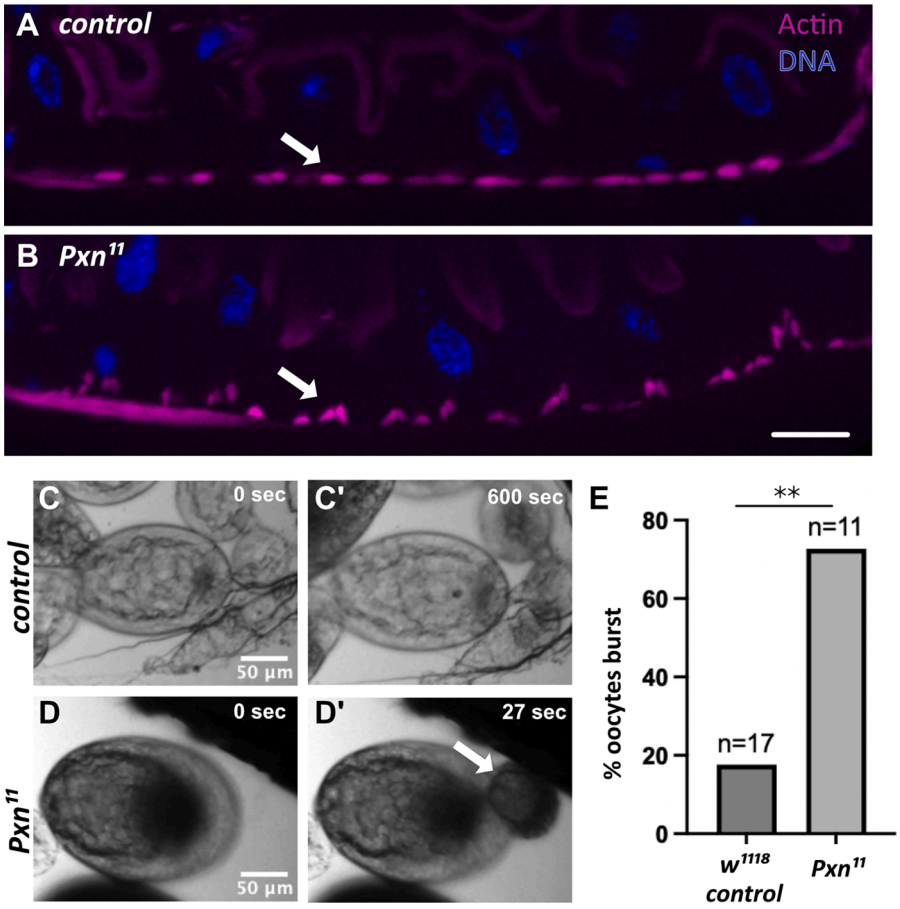

Fig. 6. Pxn^{11} homozygous mutants have defects in tissue mechanics.
A-B. Peristalsis muscles of the adult midgut are dysmorphic in the Pxn^{11} mutant. Muscles (arrows) are identified by actin staining in control w^{1118} (A) and Pxn^{11} homozygous mutants (B). Actin is also visible at the brush border. Scale bar: 10 µm.
C-E. When submerged in water, most control w^{1118} oocytes stretch but remain intact (C) whereas Pxn^{11} homozygous mutant oocytes frequently burst (D). Arrow indicates cytoplasm emerging from the rupture. Oocytes (stages 6-8) were placed in water for 10 min. 18 % of control w^{1118} oocytes burst whereas 73 % of Pxn^{11} mutants burst (E). Magnification is the same for panels C-D'. Significance determined by Fisher's exact test.

Continued Peroxidasin-mediated crosslinking maintains the stiffness of adult basement membranes

The fly and mouse mutants clarify that Peroxidasin establishes basement membrane stiffness in development, but they do not distinguish whether Peroxidasin continues to be required in adults. We previously found that RNAi-based knockdown of *Pxn* in adult flies phenocopied a muscle defect related to loss of stiffness, suggesting a continuing requirement for Pxn in maintaining basement membrane stiffness [24]. These results were surprising: the covalent sulfilimine bond is expected to be stable and has no known enzyme to reverse it, and Col4 itself is known to be a long-lived [27–29], so there is no expectation that Pxn would be required once the basement membrane was assembled and crosslinked in an adult animal. To quantitatively investigate the possibility of a continuing requirement for Pxn to maintain stiffness, we fed wild-type flies the Peroxidasin catalytic inhibitor Phloroglucinol (PHG) for 5 days [30], then assessed the tensional stiffness of their Malpighian (renal) tubules *ex vivo* (Fig. 7). Malpighian tubules, like kidney tubules in mouse, are simple epithelial tubes surrounded by basement membrane. For both kidney tubules and Malpighian tubules, tissue stiffness is determined by their basement membranes, as stiffness is not significantly different when cells are lysed before measuring [16, 24]. Inhibiting Peroxidasin with PHG did not visibly alter Malpighian tubule basement membranes, as assessed by EM (Fig. 7A,B), and basement membrane thickness was not changed (Fig. 7C). As predicted from our previous knockdown experiments, pharmacologically inhibiting Peroxidasin for 5 days was sufficient to significantly reduce tissue tensile stiffness by about half as determined from the slope of the stress-strain response at 10–20 % strain. These results, combined with previous knockdown results, demonstrate that Peroxidasin is needed in adults to maintain tissue stiffness.

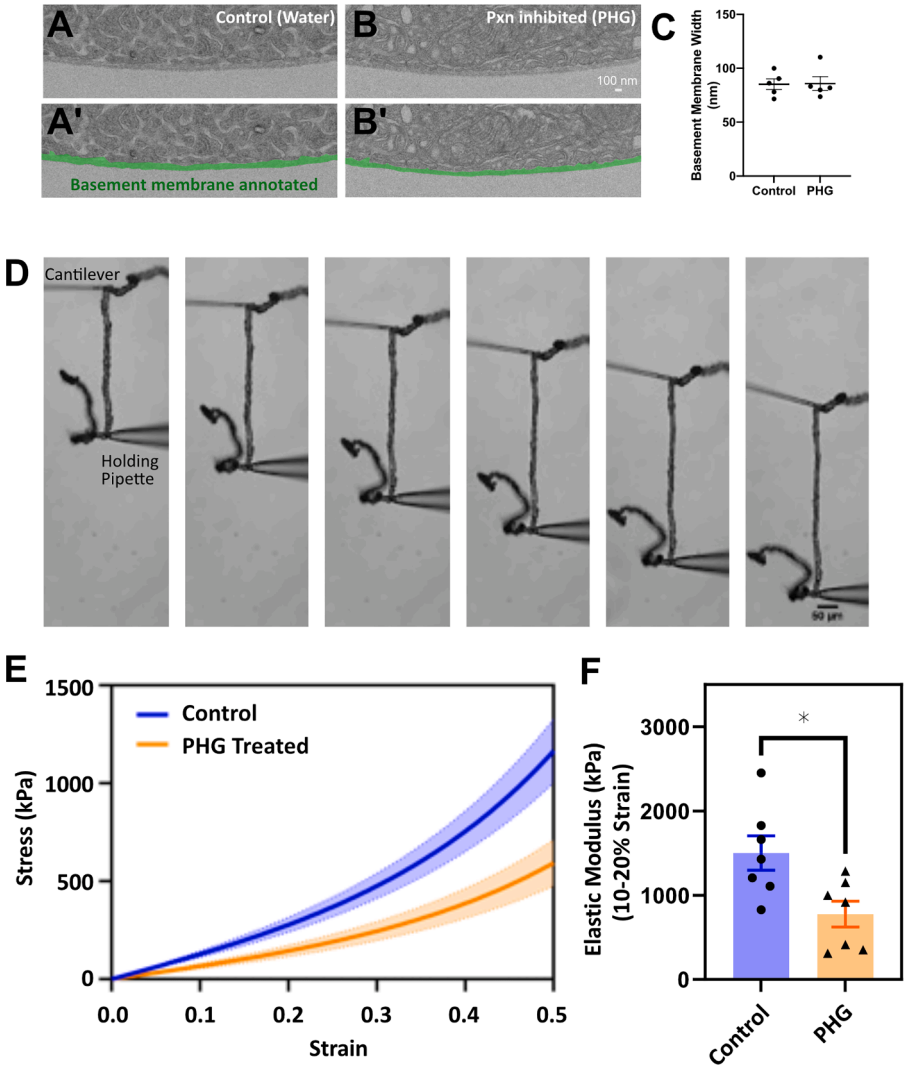

Fig. 7. Continued Peroxidasin crosslinking maintains basement membrane stiffness in adult tissues.
Malpighian (renal) tubules were dissected from adult wild-type flies that had been fed the Peroxidasin catalytic inhibitor phloroglucinol (PHG) for 5 d prior to dissection.
A-C. Transmitted electron micrograph of Malpighian tubule basement membrane shows that tubule basement membrane thickness is unchanged after 5 d Peroxidasin inhibition.
D. Tensile strain assay: Cantilever-based stiffness measurement system. Tubules were stretched between a force calibrated microcantilever and a rigid holding pipette.
E. Stress-strain curves were calculated from the bending of the cantilever and displacement of the holding pipette.
F. Elastic moduli of tubules is reduced after 5 d of Peroxidasin inhibition by PHG. Elastic modulus was calculated from slope of the stress-strain curves at 10-20 % strain. Data were analyzed by unpaired t-test in GraphPad, *$p<0.05$. See also Fig. S3.

Conclusions

Comparing fly and mouse mutations, we have shown that in both species *Peroxidasin* mutants are semi-lethal, with variable rates of escaping survivors. We note that mouse viability was assessed at weaning (~40 days after fertilization), whereas fly viability was assessed at adulthood (~10 days after fertilization), and differences in timing may contribute to the apparent reduced viability of fly vs. mouse (13 % survival to fly adulthood; 50 % survival to mouse weaning). Because even catalytic null mutations show some level of NC1 crosslinking, we conclude that there are alternative less-specific mechanisms that inefficiently crosslink the NC1 domain. It is likely that these inefficient crosslinking activities can partially substitute for Peroxidasin, resulting in incomplete rescue of lethality. Further, the fly Pxn^{11} mutants appear to be under heavy selection to accumulate suppressors, which may also contribute to the viability of otherwise lethal mutants. Analysis of the new fly catalytic null mutant Pxn^{11} demonstrates that Peroxidasin is required for tissue stiffness and to protect from tissue failure under mechanical strain. Finally, we demonstrate a requirement for Peroxidasin in maintaining adult tissue stiffness, which is surprising because the sulfilimine crosslink that Peroxidasin generates is a covalent bond without any clear mechanism for reversal. However, these results imply that either the bond must be replaced, or the collagen IV must be replaced over a period of 5 days. The findings of our study reinforce the idea that NC1 crosslinking is essential for animal life.

Methods

Fly Pxn viability analysis

Viability of transposon insertions was assessed by self-crossing *Mi(MIC}*$Pxn^{MI01492}$*/TM3* or *PBac(WH}*Pxn^{f07229}*/TM6B*. Each vial contained 15-20 virgins and 10-15 males for 2 d at 25°C before transferring to a new vial. All progeny eclosing from the vial were counted.

Pxn^{11} *deletion*

The *Peroxidasin* gene locus was targeted for mutagenesis using two guide RNAs gRNA9: GAAGCAGATCAATTCCCATT gRNA12: TGAACAGTTCCGCAGACTTC

pCFD5 plasmids were generated with each gRNA and injected into *yw; nos-Cas9 (II-attp40)* by BestGene Inc. Injected embryos were crossed to remove *Cas9* and were screened by PCR for deletions in the locus, and suspected deletions were sequenced. The Pxn^{11} deletion removes 727 base pairs, so that the predicted amino acid sequence ends at residue 1040 (isoleucine), lacking the codon for asparagine 1041. After the deletion, the last 2 bp of arginine 1283 are present generating a frame shift which results in eight nonsense mutations, the first of which occurs between leucine (L) 1297 and threonine (T) 1298.

Analysis of fly lethality through development

25-50 Pxn^{11}*/TM3,sChFP* females were crossed with half as many Pxn^{11}*/TM3,sChFP* males and placed on a grape juice plate in an egg collection cage at room temperature for one hour before moving them to a new plate supplemented with wet yeast paste for 2 hours at 25°C. After removing parents, embryos were allowed to age overnight at 18°C until roughly stage 13-15. Embryos were sorted by red fluorescence and embryos with visible development were placed on new grape plates supplemented with wet yeast paste, up to 50 embryos per plate. Every subsequent day, progeny were transferred to new grape plates supplemented with wet yeast paste and progeny were counted and developmental stage observed. At pupariation, progeny were transferred from plates to fresh vials with molasses cornmeal food to eclose and were observed daily, including counting adults. Adult phenotype was confirmed to match the appropriate genotype. The percent lost at each stage only included progeny observed at both developmental stages. For assessing pupal development, *Pxn* heterozygotes were crossed and the progeny allowed to develop in the vial. After day 6 when pupae became visible, individual pupae were tracked daily through eclosion and noted for body shape and eye color. Grape plates were made by autoclaving 700 mL dH2O and 30g agar, cooling it slightly, mixing in 300 mL Welch's grape juice and 20 mL 2.5 % Tegosept, and pouring the mixture into 60 mm Petri dishes to cool, stored at 4°C. Wild-type controls were w^{1118}.

Analysis of mouse lethality

The *K01* allele was previously described [16]. *K02* allele was generated from the *K01* allele by crossing sequentially to Flp and Cre recombinase lines as described [20], thus permanently eliminating exon 9 from the genome. Outcrossing to both the 129S2 or C57/B6 lines was done for ten generations. Genotypes of progeny were determined by PCR of tail clips of pups post-weaning.

NC1 Western blotting

50 frozen flies of two genotypes, Pxn^{11} or w^{1118}, were ground in liquid nitrogen in microfuge tubes then sonicated in 800 µl DOC buffer (10 mM Tris-Cl pH 7.5, 1 M 1 % sodium deoxycholate, 1 mM EDTA-Na, pH 8) vortexed and ground again, then incubated on ice with occasional vortexing for 30 min. Tubes were spun 4° for 30 min in a microfuge, and pellets were resuspended in 800 µl collagenase buffer (100 mM NaCl, 50 mM Tris-Cl pH 7.5, 5 mM CaCl2, 25 mM aminocaproic acid, 5 mM Benzamidine) on ice, then vortexed, spun again at 4°, resuspended in 100 µl collagenase buffer. 15 µl collagenase was added from a freshly thawed aliquot, mixed, then incubated overnight at 37°. This collagenase digest was spun 40 min at full speed at 4°, and the supernatant was removed with a gel-loading fine tip pipet to a new tube. Any remaining debris was spun out and supernatant was mixed with 1X sample buffer without DTT, boiled 60 min, analyzed by SDS-PAGE, transferred to nitrocellulose and allowed to air-dry overnight at RT, then re-wet in PBS. Primary antibody was rabbit anti-fly NC1 (1:500) (McCall et al) and secondary was LICOR anti-rabbit prepared according to manufacturer's instructions. About 1.9 fly equivalents are loaded in the 1X lanes.

Gut imaging

Optical cross sections of the adult Drosophila posterior midgut were obtained as previously described [24].

Oocyte bursting

Pxn^{11} and w^{1118} females were aged 5-7 days at 25°C on normal food. Ovaries were dissected in cold Schneider's media then transferred to a glass microscope slide with a 26×16×0.15 mm spacer (iSpacer from SunJin Lab) containing 75 µl water, then covered with a 24×40mm cover slip. Movies were taken with 5x objective on Zeiss Apotome M2 for 10 minutes, with images taken every 3 seconds.

Electron microscopy

Malpighian tubule samples were processed for transmission electron microscopy (TEM) and imaged in the Vanderbilt Cell Imaging Shared Resource-Research EM facility, as described in Howard et al., 2019. Basement membrane thickness was measured by applying a grid over the image in FIJI and measuring the thickness of the basement membrane each time the grid intersected. Each data point represents a mean of 10–70 replicate measurements.

Stiffness measurements of Malpighian tubule basement membrane

Flies were fed 100 μM PHG or water equivalent mixed in 0.2 g peach baby food (Gerber) in an Eppendorf tube cap. The cap of food was taped into an egg laying cage, and 15-20 aged and mated female flies were added along with a few males. The cages were placed in a humidified chamber at 29°C. The food was replaced and the chambers were washed daily for 5 days. Malpighian tubules were microdissected and then transferred to cold PBS. The stiffness of native and phloroglucinol (PHG) treated Malpighian tubule basement membrane was characterized using a cantilever-based tensile stiffness measurement system described previously [31]. We showed in prior studies that the cellular contribution to the overall tubule stiffness is minimal, so the measured stiffness represents the stiffness of basement membrane [16,24]. Cantilever stiffness sensors were fabricated from glass capillary tubes using a pipette puller and cantilever spring constants were calibrated in a manner similar to Shimamoto and Kapoor [32]. Malpighian tubules were attached to the cantilever and a rigid holding pipette, shown in Fig. 7. The movement of the holding pipette was controlled by a micromanipulator at a speed of 10 μm/sec to stretch the tubule and imaged in increments of 40 μm displacements. Images were captured with a digital camera attached to an inverted microscope (VWR) at 4× magnification. Displacement of the cantilever and holding pipette were analyzed in WINanalyze software. The stress was calculated as the applied force divided by the cross-sectional area of the basement membrane. The average width of the basement membrane used to calculate the cross-sectional area as measured from TEM images and tubule diameter was measured by light microscopy [16,24]. To model the stress-strain response, Humphrey model was employed to fit the experimental data. The stretch ratio was taken as the ratio of the deformed tubule length to the initial length [31, 33] and the strain = stretch ratio-1. The equations for the hyper-elastic model were used in the functional form described by Martins et al [34]. The Humphrey model was fit to the experimental data using lsqcurvefit function and the elastic moduli were calculated from the slope of the stress strain response for strain from 10 to 20 %. Representative curve fits to the experimental data and the model fit parameters are provided in the supplementary data (Fig. S3).

Data availability

Data will be made available on request.

Acknowledgements

We are grateful to Hui-Yu Ku for help with the oocyte bursting assay. This work was supported by National Institutes of Health grants F31GM148021 to AMS, R01DK116964 to GB, and R01GM137595 to APM; a Ben J. Lipps Research Fellowship from American Society of Nephrology to DW; and by National Science Foundation CAREER award 2216394 to NF.

Supplementary materials

Supplementary material associated with this article can be found, in the online version, at doi:10.1016/j.matbio.2023.11.005.

References

[1] R. Jayadev, D.R. Sherwood, Basement membranes, Curr. Biol. 27 (6) (2017) R207–R211.
[2] W. Ramos-Lewis, A. Page-McCaw, Basement membrane mechanics shape development: lessons from the fly, Matrix Biol. J. Int. Soc. Matrix Biol. (2018).
[3] W. Ramos-Lewis, K.S. LaFever, A. Page-McCaw, A scar-like lesion is apparent in basement membrane after wound repair *in vivo*, Matrix Biol. 74 (C) (2018) 101–120.
[4] J.C. Pastor-Pareja, T. Xu, Shaping cells and organs in Drosophila by opposing roles of fat body-secreted Collagen IV and perlecan, Dev. Cell 21 (2) (2011) 245–256.
[5] D.P. Keeley, E. Hastie, R. Jayadev, L.C. Kelley, Q. Chi, S.G. Payne, J.L. Jeger, B. D. Hoffman, D.R. Sherwood, Comprehensive endogenous tagging of basement membrane components reveals dynamic movement within the matrix scaffolding, Dev. Cell 54 (1) (2020) 60–74, e7.
[6] C.F. Cummings, V. Pedchenko, K.L. Brown, S. Colon, M. Rafi, C. Jones-Paris, E. Pokydeshava, M. Liu, J.C. Pastor-Pareja, C. Stothers, I.A. Ero-Tolliver, A. S. McCall, R. Vanacore, G. Bhave, S. Santoro, T.S. Blackwell, R. Zent, A. Pozzi, B. G. Hudson, Extracellular chloride signals collagen IV network assembly during basement membrane formation, J. Cell Biol. 213 (4) (2016) 479–494.
[7] J.A. Summers, M. Yarbrough, M. Liu, W.H. McDonald, B.G. Hudson, J.C. Pastor-Pareja, S.P. Boudko, Collagen IV of basement membranes: IV. Adaptive mechanism of collagen IV scaffold assembly in Drosophila, J. Biol. Chem. (2023), 105394.
[8] R. Vanacore, A.J.L. Ham, M. Voehler, C.R. Sanders, T.P. Conrads, T.D. Veenstra, K. B. Sharpless, P.E. Dawson, B.G. Hudson, A sulfilimine bond identified in collagen IV, Science 325 (5945) (2009) 1230–1234.
[9] R.E. Nelson, L.I. Fessler, Y. Takagi, B. Blumberg, D.R. Keene, P.F. Olson, C. G. Parker, J.H. Fessler, Peroxidasin: a novel enzyme-matrix protein of Drosophila development, EMBO J. 13 (15) (1994) 3438–3447.
[10] R. Shi, Z. Cao, H. Li, J. Graw, G. Zhang, V.J. Thannickal, G. Cheng, Peroxidasin contributes to lung host defense by direct binding and killing of gram-negative bacteria, PLoS Pathog. 14 (5) (2018), e1007026.
[11] A.L. Fidler, R.M. Vanacore, S.V. Chetyrkin, V.K. Pedchenko, G. Bhave, V.P. Yin, C. L. Stothers, K.L. Rose, W.H. McDonald, T.A. Clark, D.B. Borza, R.E. Steele, M.T. Ivy, J.K.H Aspirnauts, B.G. Hudson, A unique covalent bond in basement membrane is a primordial innovation for tissue evolution, Proc. Natl. Acad. Sci. 111 (1) (2014) 331–336.
[12] X. Yan, S. Sabrautzki, M. Horsch, H. Fuchs, V. Gailus-Durner, J. Beckers, M. Hrabě de Angelis, J. Graw, Peroxidasin is essential for eye development in the mouse, Hum. Mol. Genet. 23 (21) (2014) 5597–5614.
[13] H.K. Kim, K.A. Ham, S.W. Lee, H.S. Choi, H.S. Kim, H.K. Kim, H.S. Shin, K.Y. Seo, Y. Cho, K.T. Nam, I.B. Kim, Y.A. Joe, Biallelic deletion of Pxdn in mice leads to anophthalmia and severe eye malformation, Int. J. Mol. Sci. 20 (24) (2019) 6144.
[14] K. Khan, A. Rudkin, D.A. Parry, K.P. Burdon, M. McKibbin, C.V. Logan, Z. I. Abdelhamed, J.S. Muecke, N. Fernandez-Fuentes, K.J. Laurie, M. Shires, R. Fogarty, I.M. Carr, J.A. Poulter, J.E. Morgan, M.D. Mohamed, H. Jafri, Y. Raashid, N. Meng, H. Piseth, C. Toomes, R.J. Casson, G.R. Taylor, M. Hammerton, E. Sheridan, C.A. Johnson, C.F. Inglehearn, J.E. Craig, M. Ali, Homozygous mutations in PXDN cause congenital cataract, corneal opacity, and developmental glaucoma, Am. J. Hum. Genet. 89 (3) (2011) 464–473.
[15] A. Choi, R. Lao, P. Ling-Fung Tang, E. Wan, W. Mayer, T. Bardakjian, G.M. Shaw, P. Y. Kwok, A. Schneider, A. Slavotinek, Novel mutations in PXDN cause microphthalmia and anterior segment dysgenesis, Eur. J. Hum. Genet. 23 (3) (2015) 337–341.
[16] G. Bhave, S. Colon, N. Ferrell, The sulfilimine cross-link of collagen IV contributes to kidney tubular basement membrane stiffness, Am. J. Physiol. Renal Physiol. 313 (3) (2017) F596–F602.
[17] G.P. Lunstrum, H.P. Bächinger, L.I. Fessler, K.G. Duncan, R.E. Nelson, J.H. Fessler, Drosophila basement membrane procollagen IV. I. Protein characterization and distribution, J. Biol. Chem. 263 (34) (1988) 18318–18327.
[18] Y. Matsubayashi, A. Louani, A. Dragu, B.J. Sanchez-Sanchez, E. Serna-Morales, L. Yolland, A. Gyoergy, G. Vizcay, R.A. Fleck, J.M. Heddleston, T.L. Chew, D. E. Siekhaus, B.M. Stramer, A moving source of matrix components is essential for De novo basement membrane formation, Curr. Biol. 27 (22) (2017) 3526–3534, e4.
[19] M. Soudi, M. Zamocky, C. Jakopitsch, P.G. Furtmüller, C. Obinger, Molecular evolution, structure, and function of peroxidasins, Chem. Amp Biodivers. 9 (9) (2012) 1776–1793.
[20] W.C. Skarnes, B. Rosen, A.P. West, M. Koutsourakis, W. Bushell, V. Iyer, A. O. Mujica, M. Thomas, J. Harrow, T. Cox, D. Jackson, J. Severin, P. Biggs, J. Fu, M. Nefedov, P.J. de Jong, A.F. Stewart, A. Bradley, A conditional knockout resource for the genome-wide study of mouse gene function, Nature 474 (7351) (2011) 337–342.
[21] C. He, W. Song, T.A. Weston, C. Tran, I. Kurtz, J.E. Zuckerman, P. Guagliardo, J. H. Miner, S.V. Ivanov, J. Bougoure, B.G. Hudson, S. Colon, P.A. Voziyan, G. Bhave, L.G. Fong, S.G. Young, H. Jiang, Peroxidasin-mediated bromine enrichment of basement membranes, Proc. Natl. Acad. Sci. U. S. A. 117 (27) (2020) 15827–15836.
[22] S.P. Boudko, V.K. Pedchenko, E.N. Pokidysheva, A.M. Budko, R. Baugh, P. T. Coates, A.L. Fidler, H.M. Hudson, S.V. Ivanov, C. Luer, T. Pedchenko, R. L. Preston, M. Rafi, R. Vanacore, G. Bhave, J.K. Hudson, B.G. Hudson, Collagen IV of basement membranes: III. Chloride pressure is a primordial innovation that drives and maintains the assembly of scaffolds, J. Biol. Chem. (2023), 105318.
[23] A.S. McCall, C.F. Cummings, G. Bhave, R. Vanacore, A. Page-McCaw, B.G. Hudson, Bromine is an essential trace element for assembly of collagen IV scaffolds in tissue development and architecture, Cell 157 (6) (2014) 1380–1392.
[24] A.M. Howard, K.S. LaFever, A.M. Fenix, C.R. Scurrah, K.S. Lau, D.T. Burnette, G. Bhave, N. Ferrell, A. Page-McCaw, DSS-induced damage to basement membranes is repaired by matrix replacement and crosslinking, J. Cell Sci. 132 (7) (2019) jcs.226860-24.
[25] K.P. Campbell, Three muscular dystrophies: loss of cytoskeleton-extracellular matrix linkage, Cell 80 (5) (1995) 675–679.
[26] J. Crest, A. Díz-Muñoz, D.Y. Chen, D.A. Fletcher, D. Bilder, Organ sculpting by patterned extracellular matrix stiffness, eLife (2017).
[27] M.L. Decaris, M. Gatmaitan, S. FlorCruz, F. Luo, K. Li, W.E. Holmes, M. K. Hellerstein, S.M. Turner, C.L. Emson, Proteomic analysis of altered extracellular matrix turnover in bleomycin-induced pulmonary fibrosis, Mol. Cell. Proteom. 13 (7) (2014) 1741–1752.

[28] P. Liu, S.L. Edassery, L. Ali, B.R. Thomson, J.N. Savas, J. Jin, Long-lived metabolic enzymes in the crystalline lens identified by pulse-labeling of mice and mass spectrometry, eLife 8 (2019) e50170.
[29] P. Liu, X. Xie, J. Jin, Isotopic nitrogen-15 labeling of mice identified long-lived proteins of the renal basement membranes, Sci. Rep. 10 (1) (2020) 5317.
[30] G. Bhave, C.F. Cummings, R.M. Vanacore, C. Kumagai-Cresse, I.A. Ero-Tolliver, M. Rafi, J.S. Kang, V. Pedchenko, L.I. Fessler, J.H. Fessler, B.G. Hudson, Peroxidasin forms sulfilimine chemical bonds using hypohalous acids in tissue genesis, Nat. Chem. Biol. 8 (9) (2012) 784–790.
[31] S. Sant, D. Wang, R. Agarwal, S. Dillender, N. Ferrell, Glycation alters the mechanical behavior of kidney extracellular matrix, Matrix Biol. Plus 8 (2020), 100035.
[32] Y. Shimamoto, T.M. Kapoor, Microneedle-based analysis of the micromechanics of the metaphase spindle assembled in Xenopus laevis egg extracts, Nat. Protoc. 7 (5) (2012) 959–969.
[33] S. Sant, D. Wang, M. Abidi, G. Walker, N. Ferrell, Mechanical characterization of native and sugar-modified decellularized kidneys, J. Mech. Behav. Biomed. Mater. 114 (2021), 104220.
[34] P.A.L.S. Martins, R.M.N. Jorge, A.J.M. Ferreira, A comparative study of several material models for prediction of hyperelastic properties: application to silicone-rubber and soft tissues, Strain 42 (3) (2006) 135–147.